ON THE UNCERTAINTY C OMPONENTS IN SPECTRAL ANALYSIS OF BI -TONE WAVEFORMS ARISING FROM THE VIRTUAL TIME-DOMAIN APPROACH

Lorenzo Peretto [1, a], *Renato Sasdelli* [1, b], *Roberto Tinarelli* [1, c]

(1) Dipartimento di Ingegneria Elettrica, University of Bologna,
Viale Risorgimento 2, I-40136 Bologna, Italy
[a] Phone +39 0512093483 Fax +39 0512093470 e-mail: lorenzo.peretto@mail.ing.unibo.it
[b] Phone +39 0512093482 Fax +39 0512093470 e-mail: renato.sasdelli@mail.ing.unibo.it
[c] Phone +39 0512093471 Fax +39 0512093470 e-mail: roberto.tinarelli@mail.ing.unibo.it

Abstract–*Multi-tone signals are discrete-spectrum signals with spectral components located at non-harmonically related frequencies. Their spectral analysis can be performed in short observation intervals by means of a method that combines the use of a virtual time domain and statistical techniques. The contributions to uncertainty that specifically arise from the implementation of the method are discussed in the paper and a study is developed to optimize the measurement technique in the case of bi-tone, periodic or not, signals. Finally, experimental results, which confirm theory, are reported and discussed.*

Keywords - Uncertainty analysis; Multi-tone waveforms; Random sampling; Digital signal processing; Statistical analysis.

1. INTRODUCTION

Discrete-spectrum signals with components located at frequencies not harmonically related to the industrial frequency are a special case of *almost-periodic* functions, in the sense of Bohr [1], and are usually referred to as *multi-tone*. They can be periodic or nonperiodic. Multi-tone voltages and currents can be observed in electrical circuits with time-varying loads in steady-state operation.

The traditional digital techniques for periodic-signal analysis use short observation intervals and can therefore lack accuracy when applied to multi-tone signals. For instance, if the conventional Discrete Fourier Transform (DFT) algorithm is implemented, leakage effects occur.

Windowing techniques are very often implemented to overcome this problem, see e.g. [2-9].

A different approach, which allows using finite observation intervals even in the analysis of nonperiodic multi-tone signals, was proposed by the authors in [10-11]. It combines the use of a virtual time-domain (which allows exploiting the DFT algorithm advantages) and statistical techniques so that leakage effects and aliasing are reduced. However, the implementation of the approach proposed gives rise to specific components of uncertainty that will be discussed in this paper. In particular, a study will be developed to optimize the measurement technique in the case of bi-tone signals. Finally, the results of some experimental work for the theory validation will be reported and discussed in this paper.

Investigation supported by the University of Bologna (Funds for selected research topics).

2. THEORETICAL BACKGROUND

Let us consider a nonlinear circuit forced by m tone generators and denote by $\{\omega_j\}$ the set of the fundamental angular frequencies of the tones (j is $1 \le j \le m$). Let also be $\omega_j = 2\pi/T_j = 2\pi f_j$, where T_j and f_j are the period and the fundamental frequency, respectively, of the generic tone. The generic multi-tone signal $x(t)$ forced by the above tones can be expressed by means of the following equation:

$$x(t) = \sum_{n_1=-H_1}^{H_1} \dots \sum_{n_j=-H_j}^{H_j} \dots \sum_{n_m=-H_m}^{H_m} \underline{X}_{n_1 \dots n_j \dots n_m} \cdot \mathrm{e}^{\mathrm{j}(n_1\omega_1 + \dots + n_j\omega_j + \dots + n_m\omega_m)t} . \quad (1)$$

If (1) contains spectral components located at non-rational frequencies, it is referred to as *quasi-periodic.* In (1), the complex quantity $\underline{X}_{n_1 \dots n_j \dots n_m} = \underline{X}^*_{-n_1 \dots -n_j \dots -n_m}$ (the asterisk denotes the complex conjugate) is the generic Fourier coefficient relevant to the angular frequency $n_1\omega_1 + \dots + n_j\omega_j + \dots + n_m\omega_m$, the elements of the set $\{n_j\}$ are integer, whereas those of $\{H_j\}$ are natural numbers.

The virtual signal $x(\tau_1, \dots, \tau_j, \dots, \tau_m)$, defined as follows:

$$x(\tau_1, \dots, \tau_j, \dots, \tau_m) \stackrel{\Delta}{=} \sum_{n_1=-H_1}^{H_1} \dots \sum_{n_j=-H_j}^{H_j} \dots \sum_{n_m=-H_m}^{H_m} \underline{X}_{n_1 \dots n_j \dots n_m} \mathrm{e}^{\mathrm{j}n_1\omega_1\tau_1} \dots \mathrm{e}^{\mathrm{j}n_j\omega_j\tau_j} \dots \mathrm{e}^{\mathrm{j}n_m\omega_m\tau_m} , \quad (2)$$

is periodic in each virtual coordinate $\tau_1, \dots \tau_m$. If it is: $\tau_1 = \dots \tau_m = t$, (2) represents the actual signal (1); hence, the

spectral components of (1) can be determined by applying the Fourier Transform to the signal (2) in each virtual coordinate. The spectral analysis of discrete-spectrum, even nonperiodic, signals can therefore be performed by using short observation intervals T_O, in the order of those used by the commercial instruments.

In many practical situations, the electrical power systems can be modeled by means of nonlinear circuits forced by bi-tone generators. This could be, for instance, the case of power systems containing static converters. Let us consider the generic virtual bi-tone signal:

$$x(\tau_1,\tau_2) \stackrel{\Delta}{=} \sum_{n_1=-H_1}^{H_1} \sum_{n_2=-H_2}^{H_2} \underline{X}_{n_1 n_2} \mathrm{e}^{\mathrm{j}n_1\omega_1\tau_1} \mathrm{e}^{\mathrm{j}n_2\omega_2\tau_2} . \quad (3)$$

If the so-called virtual time-domain approach is used [11], the generic spectral component of (3) can be determined according to the following equation:

$$\underline{X}_{n_1 n_2} = \frac{1}{T_1} \int_{-T_1/2}^{T_1/2} \left\{ \frac{1}{T_2} \int_{-T_2/2}^{T_2/2} x(\tau_1,\tau_2) \mathrm{e}^{-\mathrm{j}n_2\omega_2\tau_2} \mathrm{d}\tau_2 \right\} \mathrm{e}^{-\mathrm{j}n_1\omega_1\tau_1} \mathrm{d}\tau_1 . \quad (4)$$

In (4), T_1 and T_2 are the periods of the tones, which are periodic in the virtual coordinate τ_1 and τ_2, respectively.

To implement (4), x is first sampled at regular time intervals equal to T_2 within T_O and starting from a given instant, which we denote by θ_2, thus acquiring a sequence of length N_a. This procedure turns into a sampling strategy such that (3) is acquired at regular time intervals in the virtual coordinate τ_2. Since the two tones are not harmonically related, this can lead to a random sampling of (3) in the virtual coordinate τ_1. If the two tones are non-commensurable, this condition of random sampling is intrinsically met, otherwise the autocorrelation matrix must be analyzed [12]. Performing a random sampling in τ_1 is a necessary condition to get consistent and efficient estimates of the spectral components (4). As soon as the acquisition process ends, a nonperiodic finite-length sequence denoted by $x_{\theta 2}[h] = x(\theta_2, hT_2)$, with h integer, is got, which is a function of a random variable. If θ_2 is varied within a time interval equal to T_2 so that $\theta_2 = kT_S$ (T_S being the sampling period and k an integer) the estimate $\underline{\tilde{X}}_{\hat{n}_1\hat{n}_2}$ of the spectral component $\underline{X}_{\hat{n}_1\hat{n}_2}$ is then given by the following equation:

$$\underline{\tilde{X}}_{\hat{n}_1\hat{n}_2} = \frac{T_S}{T_2} \frac{1}{N} \sum_{k=0}^{T_2/T_S-1} \sum_{h\in\{h\}} x_{\theta_2}[h] \mathrm{e}^{-\mathrm{j}\hat{n}_1\omega_1 hT_2} \mathrm{e}^{-\mathrm{j}\hat{n}_2\omega_2 kT_S} \quad (5)$$

where N is the nonperiodic-sequence length, $\hat{n}_1$ and $\hat{n}_2$ refer to given values of n_1 and n_2, respectively.

In practical situations, the actual values of the fundamental frequencies of both tones could not be known. It was shown in [13] that knowing approximate frequency values, such as the nominal ones, is enough to perform the spectral analysis of a bi-tone signal.

3. UNCERTAINTY ANALYSIS

Besides the effects of well-known contributions, such as gain, nonlinearity, quantization, noise, the uncertainty in spectral-components estimate (5) also depends on other sources that are intrinsic in the method implementation. They mainly are:

- a kind of time jitter, which affects the first exponential in (4) and occurs when the ratio T_S/T_2 is not integer. In this case, the generic sample is acquired at an instant that differs from the theoretical instant hT_2 by a quantity randomly changing in value and sign. This jitter can be treated as a random variable and turns into a contribution to uncertainty that, for convenience, we refer to as Type A standard uncertainty, in accordance with [14]. It can be avoided if a clock signal is available to trigger the acquisition process with the period T_2. Otherwise, it can be reduced by increasing either the sampling rate or the sequence length N.
- A contribution arising when either f_1 or f_2, or both, are not exactly known. The nature of this contribution depends on whether f_S is multiple of f_2 or not. In the former case, it is similar to a leakage effect. If f_S is not multiple of f_2, this turns into leakage and jitter effects on the spectral-components estimates.
- A further contribution to uncertainty arises from the statistical procedure adopted and is given by the variance associated to the spectral-component estimate. This Type A standard uncertainty represents the lower limit of uncertainty of the method proposed.

To optimize the measurement strategy of $\underline{X}_{\hat{n}_1\hat{n}_2}$ it is therefore necessary that f_2 is known, or the relevant clock is available to trigger the acquisition process, and that the sampling frequency is a multiple of f_2. The method implementation described in the following Section will meet the above conditions. Therefore, the study will mainly be focused on the Type A standard uncertainty associated to the variance of the spectral-component estimate.

The statistical properties (expected value $\mathrm{M}\{\underline{\tilde{X}}_{\hat{n}_1\hat{n}_2}\}$ and variance $\mathrm{Var}\{\underline{\tilde{X}}_{\hat{n}_1\hat{n}_2}\}$) of the above spectral-component estimates will therefore be investigated in this paper. It will be shown in the Appendix that the expected value and the variance of the estimate $\frac{1}{N}\sum_{h\in\{h\}} x_{\theta_2}[h]\mathrm{e}^{-\mathrm{j}\hat{n}_1\omega_1 hT_2}$, which appears in (5) and is denoted by the symbol $\underline{\tilde{X}}_{\hat{n}_1}$, are given by the equations (6) and (7):

$$\mathrm{M}\{\underline{\tilde{X}}_{\hat{n}_1}\} = \sum_{n_1=-H_1}^{H_1} \underline{X}_{n_1} \mathrm{sinc}[f_1 AT_2 \cdot (n_1-\hat{n}_1)] \frac{\mathrm{sinc}[f_1 NAT_2(n_1-\hat{n}_1)]}{\mathrm{sinc}[f_1 T_2 A(n_1-\hat{n}_1)]} \mathrm{e}^{\mathrm{j}\pi f_1 AT_2(n_1-\hat{n}_1)(N-2)}, \quad (6)$$

$$\mathrm{Var}\{\underline{\tilde{X}}_{\hat{n}_1}\}=\frac{1}{N^2}\sum_{n_1=-H_1}^{H_1}\sum_{m_1=-H_1}^{H_1}\sum_{h=0}^{N-1}\sum_{k=0}^{N-1}\underline{X}_{n_1}\underline{X}^{*}_{m_1}\mathrm{e}^{\mathrm{j}2\pi f_1 AT_2 h(n_1-\hat{n}_1)}\mathrm{e}^{-\mathrm{j}2\pi f_1 AT_2 k(m_1-\hat{n}_1)}\cdot$$
$$\cdot\mathrm{M}\left\{\mathrm{e}^{\mathrm{j}2\pi f_1 T_2(n_1-\hat{n}_1)y_\mathrm{h}}\cdot\mathrm{e}^{-\mathrm{j}2\pi f_1 T_2(m_1-\hat{n}_1)y_\mathrm{k}}\right\}-$$
$$-\frac{1}{N}\sum_{n_1=-H_1}^{H_1}\sum_{h=0}^{N-1}\underline{X}_{n_1}\mathrm{e}^{\mathrm{j}2\pi f_1 AT_2 h(n_1-\hat{n}_1)}\cdot\mathrm{M}\left\{\mathrm{e}^{\mathrm{j}2\pi f_1 T_2(n_1-\hat{n}_1)y_\mathrm{h}}\right\}\cdot\mathrm{M}\{\underline{\tilde{X}}_{\hat{n}_1}\}- \quad (7)$$
$$-\frac{1}{N}\sum_{n_1=-H_1}^{H_1}\sum_{h=0}^{N-1}\underline{X}^{*}_{n_1}\mathrm{e}^{-\mathrm{j}2\pi f_1 AhT_2(n_1-\hat{n}_1)}\cdot\mathrm{M}\left\{\mathrm{e}^{-\mathrm{j}2\pi f_1 T_2(n_1-\hat{n}_1)y_\mathrm{h}}\right\}\mathrm{M}\{\underline{\tilde{X}}_{\hat{n}_1}\}+$$
$$+\mathrm{M}\{\underline{\tilde{X}}_{\hat{n}_1}\}\cdot\mathrm{M}\{\underline{\tilde{X}}_{\hat{n}_1}\}^{*}.$$

In (7), y_h is a random integer variable. It is then possible to determine how the component (7) of uncertainty propagates through the DFT algorithm to affect the estimate (5). It is worthwhile noting that $\underline{\tilde{X}}_{\hat{n}_1}$ is asymptotically unbiased. If the condition of independent random variables is not met, so that the estimates (5) are biased, or the sequence length N is not properly chosen, the effect of this Type A standard uncertainty can exceed that of all other error sources.

4. EXPERIMENTAL WORK

Experiments were carried out to both verify the theory leading to (6) and (7) and test the performance of the method. To this purpose, the spectral analysis of a bi-tone signal was simulated, since simulations have the advantage of providing reference signals with exactly known parameters.

In the simulations, the signal was acquired with a sampling frequency f_S=100kSa/s to get a sequence of length N_a. A sub-set of data was then built by extracting from the above sequence all the samples relevant to instants spaced of a time interval equal to the smaller between the two tone periods (we assume it is T_2). Finally, the elements of the nonperiodic sequence $x_{\theta 2}[h]$ were randomly extracted from the above sub-set, according to a suitable law, in such a way that the generic k-th element corresponds to the instant t_k given by the following equation:

$$t_\mathrm{k}=(A\cdot k+y_\mathrm{k})\cdot T_2, \quad (8)$$

where: k=1, 2, …, N_p; N_p refers to the number of processed data; A is a suitable natural even number (which allows to randomize the choice of t_k) and y_k a random integer variable with uniform distribution in [–A/2, + A/2]. On average, the value of N_p is equal to N_a/A. If we impose y_k = 0, a leakage effect arising from the fact that f_S and T_1 are asynchronous could affect the estimate of $\underline{\tilde{X}}_{n_1 n_2}$.

As for the signal waveforms, two simple cases of voltage bi-tone signals were first considered and analyzed. Both were given by the sum of two sinusoidal tones according to the following equation:

$$u(t)=U_1\cos(2\pi f_1 t+\varphi_1)+U_2\cos(2\pi f_2 t+\varphi_2). \quad (9)$$

In the case #1, the tone frequencies were: f_1=52.125 Hz and f_2=4 kHz; the signal in the case #2 only differs from the previous one because of the frequency value of tone 1, which was taken f_1 =30.1$\sqrt{3}$ Hz = 52.134729..Hz. Hence, the signal (9) in case #1 is periodic with period 10^3s, in case #2 is quasi-periodic.

A Monte-Carlo procedure, in which each experiment was repeated 200 times, was adopted to investigate on the expected value and variance of the spectral-component estimates.

It was verified, as it is shown in Fig. 1, that taking A=2 optimizes the method performance, thus providing the lowest uncertainties in the estimates of both the amplitude and phase of the signal spectral components.

The expected values of the amplitude and phase, along with their standard deviation σ, of the tones of the signal (9), in both the cases #1 and #2, are compared to the reference ones in Tab. 1. The above results were determined by taking A=2 (hence, by processing on average $N_\mathrm{p}=N_\mathrm{a}/2=5\cdot10^4$ samples). They prove that the method performance is the same, no matter the bi-tone signal is periodic or not.

Table 1–Comparison between the results of the spectral analysis of the bi-tone signal (9) and the reference values of amplitudes and phases.

	U_1 [V]			φ_1 [rad]			U_2 [V]			φ_2 [rad]		
Case	Ref. value	Exp. value	σ	Ref. value	Exp. value	σ	Ref. value	Exp. value	σ	Ref. value	Exp. value	σ
#1	50	49.95	1.8E-2	0.5236	0.5217	3.8E-3	5	5.00	1.1E-2	0	-6E-4	2.4E-3
#2	50	49.94	1.8E-2	0.5236	0.5217	3.8E-3	5	5.00	1.4E-2	0	-7E-4	2.6E-3

Tab. 2 reports expected value and variance σ^2 of both the amplitude and phase of the tone 1 of signal (9), in the case #2. They were determined by increasing the length N_a of acquired data, i.e. by increasing the observation interval from 0.2s to 1s. Since the variance varies inversely to the number of processed samples, the Central Limit Theorem is met.

The spectral analysis of a quasi-periodic signal (case #2)

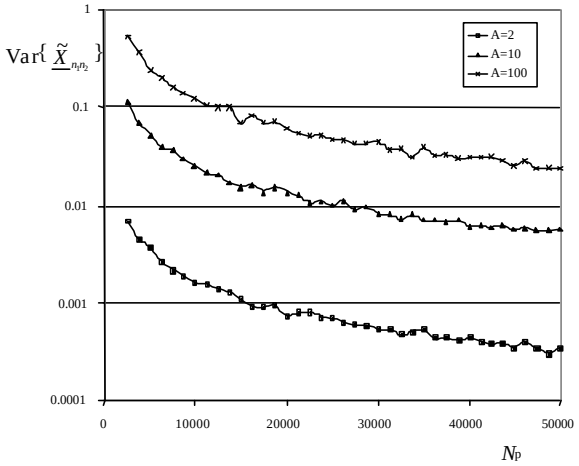

Fig. 1–Signal (9), case #2: plot of Var{ $\underline{\tilde{X}}_{\hat{n}_1\hat{n}_2}$ } vs. N_p

was also performed by assuming that the frequency f_1 was known with very poor approximation. The method performance was found to be very good in such a situation, as it is shown by the results reported at the sixth line in Tab. 2. As a matter of fact, they are the same as those determined under the assumption that f_1 is known, except for an increased phase angle error (the variance relevant to $M\{\varphi_1\}$ increased of one order of magnitude). As for the value of f_1, it can be estimated with an approximation expressed by the less significant digit of the floating point notation of the microprocessor used.

Finally, simulations were also performed under the assumption that only the nominal value, not the actual one, of f_2 was known. The results at the last line of Tab. 2 refer to a situation where it was assumed the nominal value f_2=4kHz, whereas the actual value was 3.996 kHz, which is not a submultiple of f_S.

Table 2–Signal (9), case #2: expected values of amplitude $M\{U_1\}$ and phase $M\{\varphi_1\}$ of tone 1 compared to the reference values.

	U_1 [V]			φ_1 [rad]		
Processed samples	Reference value	$M\{U_1\}$	σ^2	Reference value	$M\{\varphi_1\}$	σ^2
10000	50	49.77	$15\cdot10^{-4}$	0.5236	0.5286	$.67\cdot10^{-6}$
20000	50	49.72	$8.5\cdot10^{-4}$	0.5236	0.5259	$.33\cdot10^{-6}$
30000	50	49.75	$5.9\cdot10^{-4}$	0.5236	0.5232	$.24\cdot10^{-6}$
40000	50	49.84	$4.5\cdot10^{-4}$	0.5236	0.5217	$.18\cdot10^{-6}$
50000	50	49.94	$3.4\cdot10^{-4}$	0.5236	0.5217	$.14\cdot10^{-6}$
50000	50	49.96	$3.1\cdot10^{-4}$	0.5236	0.5228	$1.2\cdot10^{-6}$
50000	50	49.97	$3.5\cdot10^{-4}$	0.5236	0.5230	$.71\cdot10^{-6}$

Equation (7) shows that the variance of a spectral-component estimate depends on the number of the signal spectral components. The waveform of the bi-tone signal (9) was therefore modified by adding harmonics of the frequencies of the two tones. The results of simulations aimed to investigate the effect of the presence of harmonics of tone 1 (in particular: number and order of harmonic components) are reported in Tab. 3 and Tab. 4.

Table 3–Bi-tone signal, case #2: expected values of amplitude and phase of tone 1 vs. the number of its harmonic components. A=2; T_O=1s.

	U_1 [V]			φ_1 [rad]		
Number of harmonics	Ref. value	$M\{U_1\}$	σ^2	Ref. Value	$M\{\varphi_1\}$	σ^2
1	50	49.95	$4.0\cdot10^{-4}$	0.5236	0.5219	$.19\cdot10^{-6}$
2	50	49.94	$6.3\cdot10^{-4}$	0.5236	0.5223	$.21\cdot10^{-6}$
3	50	49.94	$8.5\cdot10^{-4}$	0.5236	0.5222	$.26\cdot10^{-6}$
4	50	49.93	$12\cdot10^{-4}$	0.5236	0.5223	$.27\cdot10^{-6}$
5	50	49.93	$14\cdot10^{-4}$	0.5236	0.5223	$.30\cdot10^{-6}$

An increasing number of odd-order harmonics (whose amplitudes and phases are listed in Tab. 4) was added to the tone 1. Tab. 3 shows that the variance of the estimate of the parameters of tone 1 increases as the number of harmonics increases. Tab.4 reports the results of the spectral analysis of a quasi-periodic bi-tone signal with five harmonics added to the tone 1. It shows that the variance (and, hence, σ) increases as the order h of the spectral component increases. As for the influence of the amplitude U_h of the generic harmonic component, comparing the two last lines of Tab. 4 seems to show that the variance of the phase estimate improves as the component amplitude increases.

Table4–Comparison between the reference and expected values of amplitude and phase of the spectral components added to signal (9) , case#2. A=2; T_O = 1s.

	U_h [V]		φ_h [rad]	
Component located at	Reference Value	$M\{U_h\} \pm \sigma$	Reference value	$M\{\varphi_h\} \pm \sigma$
$3\cdot f_1$	15	15.01 ± 0.06	0	$(-4 \pm 3)\cdot10^{-3}$
$5\cdot f_1$	10	9.98 ± 0.07	0	$(-7 \pm 7)\cdot10^{-3}$
$7\cdot f_1$	7	6.96 ± 0.10	0	$(-9 \pm 13)\cdot10^{-3}$
$9\cdot f_1$	5.5	5.45 ± 0.11	0	$(-3 \pm 22)\cdot10^{-3}$
$11\cdot f_1$	4.5	4.46 ± 0.15	0	$(-7 \pm 35)\cdot10^{-3}$
$11\cdot f_1$	45	44.97 ± 0.18	0	$(-0.4 \pm 4)\cdot10^{-3}$

Finally, the trends of $\mathrm{Var}\{\underline{\tilde{X}}_{\hat{n}_1}\}$, which were derived from both the theoretical model (7) and simulations performed on a quasi-periodic bi-tone signal, are plotted in Fig. 2 vs. the nonperiodic-sequence length N. The value N=2000 corresponds to an observation interval T_O=1s. Note that the above curves (like also those in the Fig. 1) are in agreement with the Central Limit Theorem.

5. CONCLUSIONS

Multi-tone signals have discrete-spectrum waveforms with spectral components located at non-harmonically related frequencies. They can be periodic or quasi-periodic; the latter case occurs when spectral components are located at frequencies expressed by non-rational numbers. A multi-tone signal can be analyzed in short observation intervals by using a virtual time-domain approach combined with a statistical technique. Specific contributions to uncertainty arise from the method implementation. They have been discussed in the paper, in the case of bi-tone signals, with the

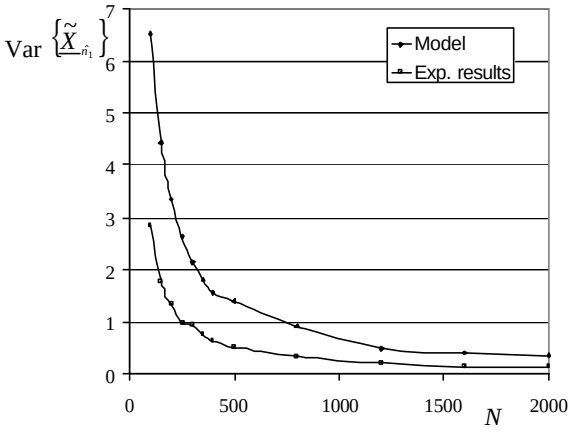

Fig. 2–Plots of $\mathrm{Var}\{\underline{\tilde{X}}_{\hat{n}_1}\}$

purpose of finding an optimal measurement strategy. It requires that the fundamental frequency of a tone is known and is a sub-multiple of the sampling frequency. When these conditions are met, the lower limit of uncertainty in spectral analysis is a Type A standard uncertainty given by the variance of the statistical mean value of the spectral-component estimate.

A study aimed at modeling the statistical properties of the above estimates has also been developed in the paper. Tests have been simulated to compare with theory the measurement results obtained both under optimal and non-optimal conditions. The simulations results confirm theory and show the very good performance of the method proposed.

6. APPENDIX

6.1 Expected value and variance of $\underline{\tilde{X}}_{\hat{n}_1}$

Since all the sampling instants are separated by a multiple of T_2, $\underline{\tilde{X}}_{\hat{n}_1}$ can be expressed by:

$$\underline{\tilde{X}}_{\hat{n}_1} = \frac{1}{N}\sum_{h=0}^{N-1} x(t_h)\mathrm{e}^{-\mathrm{j}2\pi\hat{n}_1 f_1 t_h} = \\ = \frac{1}{N}\sum_{n_1=-H_1}^{H_1}\sum_{h=0}^{N-1}\underline{X}_{n_1}\mathrm{e}^{\mathrm{j}2\pi f_1 t_h T_2(n_1-\hat{n}_1)} \qquad \text{(A1)}$$

where: $\underline{X}_{n_1} = \sum_{n_2=-H_2}^{H_2}\underline{X}_{n_1 n_2}$.

Since $t_h = (hA + y_h)T_2$, it holds:

$$\mathrm{M}\left\{\underline{\tilde{X}}_{\hat{n}_1}\right\} = \frac{1}{N}\sum_{n_1=-H_1}^{H_1}\sum_{h=0}^{N-1}\underline{X}_{n_1}\mathrm{e}^{\mathrm{j}2\pi f_1 AhT_2(n_1-\hat{n}_1)}\mathrm{M}\left\{\mathrm{e}^{\mathrm{j}2\pi f_1 y_h T_2(n_1-\hat{n}_1)}\right\} \qquad \text{(A2)}$$

Moreover, it can easily be shown that:

$$\mathrm{M}\left\{\mathrm{e}^{j2\pi f_1 y_h T_2(n_1-\hat{n}_1)}\right\} = \mathrm{sinc}(f_1 AT_2(n_1-\hat{n}_1)); \qquad \text{(A3)}$$

hence:

$$\mathrm{M}\left\{\underline{\tilde{X}}_{\hat{n}_1}\right\} = \frac{1}{N}\sum_{n_1=-H_1}^{H_1}\sum_{h=0}^{N-1}\underline{X}_{n_1}\mathrm{e}^{j2\pi f_1 AhT_2(n_1-\hat{n}_1)}\mathrm{sinc}(f_1 AT_2(n_1-\hat{n}_1))$$

$$= \sum_{n_1=-H_1}^{H_1}\underline{X}_{n_1}\mathrm{sinc}(f_1 AT_2(n_1-\hat{n}_1))\frac{1}{N}\sum_{h=0}^{N-1}\mathrm{e}^{j2\pi f_1 AhT_2(n_1-\hat{n}_1)}. \qquad \text{(A4)}$$

The last sum in (A4), which is a geometric series, gives:

$$\frac{1}{N}\sum_{h=0}^{N-1}\mathrm{e}^{\mathrm{j}2\pi f_1 AhT_2(n_1-\hat{n}_1)} = \mathrm{e}^{\mathrm{j}\pi f_1 T_2(n_1-\hat{n}_1)(N-2)}\frac{\mathrm{sinc}(f_1 NAT_2(n_1-\hat{n}_1))}{\mathrm{sinc}(f_1 AT_2(n_1-\hat{n}_1))},$$

so that (A4) provides (6).

As for the variance of $\underline{\tilde{X}}_{\hat{n}_1}$, it holds:

$$\mathrm{Var}\left\{\underline{\tilde{X}}_{\hat{n}_1}\right\} = \mathrm{M}\left\{\left|\underline{\tilde{X}}_{\hat{n}_1} - \mathrm{M}\left\{\underline{\tilde{X}}_{\hat{n}_1}\right\}\right|^2\right\} = \mathrm{M}\left\{\left|\frac{1}{N}\sum_{n_1=-H_1}^{H_1}\sum_{h=0}^{N-1}\underline{X}_{n_1}\mathrm{e}^{j2\pi f_1 AhT_2(n_1-\hat{n}_1)}\mathrm{e}^{j2\pi f_1 T_2(n_1-\hat{n}_1)y_h} - M\left\{\underline{\tilde{X}}_{\hat{n}_1}\right\}\right|^2\right\} =$$

$$= \left\{\left[\frac{1}{N}\sum_{n_1=-H_1}^{H_1}\sum_{h=0}^{N-1}\underline{X}_{n_1}\mathrm{e}^{j2\pi f_1 AhT_2(n_1-\hat{n}_1)}\mathrm{e}^{j2\pi f_1 T_2(n_1-\hat{n}_1)y_h} - \mathrm{M}\left\{\underline{\tilde{X}}_{\hat{n}_1}\right\}\right]\cdot\left[\frac{1}{N}\sum_{n_1=-H_1}^{H_1}\sum_{h=0}^{N-1}\underline{X}_{n_1}\mathrm{e}^{j2\pi f_1 AhT_2(n_1-\hat{n}_1)}\mathrm{e}^{j2\pi f_1 T_2(n_1-\hat{n}_1)y_h} - \mathrm{M}\left\{\underline{\tilde{X}}_{\hat{n}_1}\right\}\right]^*\right\}$$

which, with some steps, turns into (7).

ACNOWLEDGMENT

This work is a part of a research program supported by the University of Bologna.

REFERENCES

[1] H. Bohr: *Fastperiodische Funktionen*, Erg. Math., Springer, Berlin, 1932.

[2] V. Staudt, J. Wiesemann, "Identification of sinusoidal functions contained in a signal", in *Proc. of IEEE ICHQP VII*, Las Vegas, USA, 1996, pp. 375-380.

[3] V. Staudt, "Effects of window functions explained by signals typical to power electronics", in *Proc. of IEEE ICHQP VIII*, Athens, Greece, vol. 2, 1998, pp. 952-957.

[4] P. Carbone, E. Nunzi and D. Petri, "Sampling criteria for the estimation of multisine signal parameters", in *Proc. of IEEE IMTC/2000*, Baltimore, USA, vol. 2, 2000, pp. 636-640.

[5] F. Attivissimo, M. Savino and A. Trotta, "A study on nonlinear averaging to perform the characterization of power spectral density estimation algorithms", *IEEE Trans. Inst. Meas.*, vol. 49, No. 5, Oct. 2000, pp. 1034-1042.

[6] G. Andria, M. Savino and A. Trotta, "FFT-based algorithms oriented to measurements on multifrequency signals", *Measurement*, vol. 12, No. 1, Oct. 1993, pp. 25-42.

[7] L. Peretto, F. Filicori and R. Sasdelli, "On the definition of rms value and active power in quasi-periodic conditions", in *Proc. of XV IMEKO World Congress*, Osaka, Japan, 1999, vol. IV, pp. 43-48.

[8] J. Borkowski, "LIDFT-the DFT linear interpolation method", *IEEE Trans. Inst. Meas.*, vol. 49, No. 4, Aug. 2000, pp. 741-745.

[9] Fusheng Z., Zongxing G. and Wei Y., "The algorithm of interpolating windowed FFT for harmonic analysis of electric power system", *IEEE Trans. Power.Del.*, vol. 16, No. 2, Apr. 2001, pp. 160-164.

[10] L. Peretto, R. Sasdelli and F. Filicori, "A digital method for the characterization of power systems in the presence of multi-tone signals", in *Proc. of IEEE WISP '99*, Budapest, Hungary, 1999, pp. 116-120.

[11] L. Peretto, R. Sasdelli, "Measurements for the characterization of quasi-periodic waveforms", in *Proc. of Fifth International Workshop on Power Definitions and Measurements under Nonsinusoidal Conditions*, Milano, Italy, 2000, pp. 13-18.

[12] A. Papoulis, *Probability, Random Variables and Stochastic Processes*, McGraw-Hill, New York, USA, 1965.

[13] L. Peretto, R. Sasdelli, R. Tinarelli and C. Rossi, "Measurements on electrical power systems under bi-tone conditions by using the virtual time domain approach", in *Proc. of Fifth International Workshop on Power Definitions and Measurements under Nonsinusoidal Conditions*, Milano, Italy, 2000, pp. 137-142.

[14] *Guide to the expression of uncertainty in measurement*, ISO, International Standardization Organization, Geneva, Switzerland, 1995.